Molecular Biology of the Cell
Vol. 12, 143–154, January 2001

Amino-terminal Polypeptides of Vimentin Are Responsible for the Changes in Nuclear Architecture Associated with Human Immunodeficiency Virus Type 1 Protease Activity in Tissue Culture Cells

Robert L. Shoeman,* Claudia Hüttermann, Roland Hartig, and Peter Traub

Max-Planck-Institut für Zellbiologie, Rosenhof, D-68526 Ladenburg, Germany

Submitted August 21, 2000; Revised October 18, 2000; Accepted October 23, 2000
Monitoring Editor: Joseph Gall

Electron microscopy of human skin fibroblasts syringe-loaded with human immunodeficiency virus type 1 protease (HIV-1 PR) revealed several effects on nuclear architecture. The most dramatic is a change from a spherical nuclear morphology to one with multiple lobes or deep invaginations. The nuclear matrix collapses or remains only as a peripheral rudiment, with individual elements thicker than in control cells. Chromatin organization and distribution is also perturbed. Attempts to identify a major nuclear protein whose cleavage by the protease might be responsible for these alterations were unsuccessful. Similar changes were observed in SW 13 T3 M [vimentin$^+$] cells, whereas no changes were observed in SW 13 [vimentin$^-$] cells after microinjection of protease. Treatment of SW 13 [vimentin$^-$] cells, preinjected with vimentin to establish an intermediate filament network, with HIV-1 PR resulted in alterations in chromatin staining and distribution, but not in nuclear shape. These same changes were produced in SW 13 [vimentin$^-$] cells after the injection of a mixture of vimentin peptides, produced by the cleavage of vimentin to completion by HIV-1 PR in vitro. Similar experiments with 16 purified peptides derived from wild-type or mutant vimentin proteins and five synthetic peptides demonstrated that exclusively N-terminal peptides were capable of altering chromatin distribution. Furthermore, two separate regions of the N-terminal head domain are primarily responsible for perturbing nuclear architecture. The ability of HIV-1 to affect nuclear organization via the liberation of vimentin peptides may play an important role in HIV-1-associated cytopathogenesis and carcinogenesis.

INTRODUCTION

Fibroblasts microinjected with human immunodeficiency virus type 1 protease (HIV-1 PR) examined at the light microscopic level were found to exhibit rapid changes in nuclear morphology and chromatin organization, followed by disruption of actin-containing stress fibers and an eventual collapse of cytoplasmic vimentin intermediate filaments (IFs) (Höner *et al.*, 1991). Although the effects on the cytoplasmic cytoskeletal structures are readily explained by the cleavage of their integral or associated proteins (Shoeman *et al.*, 1990a, 1991, 1993), the events giving rise to the nuclear alterations have remained an enigma. These nuclear changes occur most rapidly at the lowest concentrations of HIV-1 PR tested (Höner *et al.*, 1991) and closely resemble those described for a variety of tissues examined in HIV-1-infected individuals (Shoeman *et al.*, 1992, for discussion and references).

Because several IF subunit proteins are excellent substrates for HIV-1 PR (Shoeman *et al.*, 1990a) and because the nuclear matrix core filaments are morphologically indistinguishable from the cytoplasmic IFs (Jackson and Cook, 1988; He *et al.*, 1990; Wang and Traub, 1991; Padros *et al.*, 1997), it seemed likely that one or more components of the nuclear matrix might be cleaved by HIV-1 PR and be responsible for the alterations in nuclear structure. Although it was possible to visualize alterations in residual cellular and nuclear structures in HIV-1 PR-treated cells, it was not possible to correlate the cleavage of a nuclear protein (e.g., NuMA; the nuclear mitotic apparatus protein) with the changes in nuclear architecture. Instead, we were able to show, by a com-

* Corresponding author. E-mail address: rshoeman@zellbio.mpg.de.

Abbreviations used: CLS microscopy, confocal laser scanning microscopy; DAPI, 4′,6-diamidino-2-phenylindole; F-, fluorescein; FITC, fluorescein isothiocyanate; HIV-1 PR, human immunodeficiency virus type 1 protease; HSF, human skin fibroblast; IF, intermediate filament; *m/z*, mass/charge; MALDI-TOF, matrix-assisted laser desorption ionization/time of flight; NT, amino terminus: NuMA, nuclear mitotic apparatus protein; TFA, trifluoroacetic acid.

bination of cell biological and biochemical approaches, that the activity of the isolated head domain of vimentin (either produced by cleavage by HIV-1 PR or purified biochemically) is both necessary and sufficient to perturb nuclear shape and disrupt chromatin organization.

MATERIALS AND METHODS

Proteins and Peptides

Vimentin was purified from mouse Ehrlich ascites tumor cells (Nelson *et al.*, 1982). Mouse vimentin has 97% sequence identity to human vimentin and yields products similar to those obtained from human vimentin when cleaved by HIV-1 PR (Shoeman *et al.*, 1990a). T-vimentin, which lacks the first 70 amino acid residues of vimentin, was prepared as described (Traub *et al.*, 1992a). The amino-terminal vimentin peptide NT1, containing residues 1–96, was prepared from mouse vimentin as previously described (Traub *et al.*, 1992b). Peptide R23R, whose sequence is identical to that of mouse vimentin (vim) residues 22 to 44 (i.e., vim_{22-44}), peptide R25R (vim_{44-68}), peptide P410 (vim_{3-22}) peptide P411 (vim_{25-44}), and peptide P412 (vim_{84-103}) were synthesized and purified (>95%) by Neosystem (Strasbourg, France) or Eurogentec (Seraing, Belgium). Peptides were dissolved either in 10 mM K-phosphate, pH 7.5, at a concentration of 2 mg/ml or in 10 mM 3-(*N*-morpholino)ethanesulfonic acid (MOPS), pH 7 at 0.2 mM for microinjection, as indicated in results. Vimentin deletion mutant proteins, lacking sequences as indicated within the N-terminal head domain, were produced by conventional recombinant DNA technology and purified from *Escherichia coli* as described (Shoeman *et al.*, 1999). For the initial experiments, purified recombinant HIV-1 PR provided by S. Roy (Hoffmann-La Roche, Nutley, NJ) was used. For the majority of the experiments, recombinant HIV-1 PR prepared in this laboratory from *E. coli* bearing the plasmid pPTΔN (Graves *et al.*, 1988; used with permission of Dr. M.C. Graves, Hoffmann-La Roche) according to a protocol supplied by S. Roy was used (details available on request). The HIV-1 PR was dialyzed against 50 mM K-phosphate, pH 7.5, 10% (vol/vol) glycerol and stored in aliquots at −196°C. As in previous experiments (Shoeman *et al.*, 1990a), this preparation was ~10% pure and control bacterial extract, a corresponding chromatography fraction from *E. coli* cells lacking the HIV-1 PR expression vector, was used as indicated for microinjection controls. Both preparations were used at a protein concentration of 70 μg/ml unless indicated otherwise. Alternatively, 10 mM MOPS, pH 7.0 or 0.1% bovine serum albumin in Ca^{2+}- and Mg^{2+}-free phosphate-buffered saline (Höner *et al.*, 1991) were used as controls. Limit digests of vimentin and mutant vimentin proteins were produced by incubating the proteins for 3–18 h with an excess of the HIV-1 PR (i.e., the amount of HIV-1 PR, determined by titration, necessary to ensure complete cleavage of the individual proteins in 1 h under standard conditions, was added to the sample mixtures that were then incubated at 37°C for 3 h or overnight). The terminal peptides produced by treatment with HIV-1 PR (which cleaves wild-type vimentin after residues 51, 60, 92, and 422 [Shoeman *et al.*, 1990a]) of vimentin and the mutant vimentin proteins were purified by reverse phase high performance liquid chromatography (HPLC) on a C18 column (Wang *et al.*, 2000). $OD_{220\ nm}$ peak fractions were concentrated by drying in a vacuum centrifugal concentrator and were resuspended in 20 μl of 0.1% trifluoroacetic acid. The mass and thus identity of each purified peptide was determined by MALDI-TOF mass spectrometry, using sinapinic acid as a matrix, performed on a Shimadzu MALDI IV instrument (Shimadzu, Duisburg, Germany), in linear, high mass, positive mode with delayed extraction, by using oxidized bovine insulin B chain and bovine ubiquitin (both from Sigma, Deisenhofen, Germany) as mass standards, essentially as described (Wang *et al.*, 2000). Observed mass/charge (*m/z*) values were accurate to >0.2%, based on the predicted values, except for peptide $vimentin_{1\text{-}\Delta(25-63)\text{-}92}$ (0.5%). The amount of each peptide recovered from the HPLC column was determined by UV-spectroscopy in a microcuvette (1-cm path length, illuminated volume ~5 μl), based on an $E_{235\ nm}$ of 1.334 for a 1-mg/ml solution of purified NT1 in 0.1% trifluoroacetic acid. The concentration of NT1 was determined as described (Shoeman *et al.*, 1999). The trifluoroacetic acid was removed by vacuum centrifugal concentration and the peptides were resuspended in 10 mM MOPS, pH 7.0 to give a final concentration of 0.2 mM. An aliquot of NT1 was dialyzed against distilled water and then processed as the other peptides to give a final concentration of 0.2 mM in 10 mM MOPS, pH 7.0 buffer (0.2 mM NT1 peptide is equivalent to 2 mg/ml). The cleavages of vimentin proteins or NuMA by HIV-1 PR could be inhibited by pepstatin A, an inhibitor of aspartyl proteases (Seelmeier *et al.*, 1988). For experiments to determine the cellular distribution of NT1 after microinjection, a mutant vimentin protein, containing a cysteine in place of $serine_1$ as the amino terminal residue, was produced by recombinant DNA technology and partially purified as described (Beuttenmüller *et al.*, 1994). This cys_1-vimentin was labeled with fluorescein-5-maleimide (Molecular Probes, Eugene, OR), essentially according to Molecular Probe's instructions, and digested with endoproteinase Lys-C (Roche Molecular Biochemicals, Mannheim, Germany) to generate a fluorescein-labeled cys_1-NT1 molecule (F-cys_1-NT1). The F-cys_1-NT1 was purified by HPLC on a C18 column and identified by MALDI-TOF, as described above. A $vimentin_{1-104}$ NT-green fluorescent protein fusion protein expression vector, in which the first 104 codons of the mouse vimentin cDNA was fused in-frame to the 5′ end of a green fluorescent protein open reading frame, also was transfected into SW 13 [vimentin$^-$] cells to localize the $vimentin_{1-104}$ NT peptide (plasmid and results kindly provided by Dr. U. Niesel, this institute). In initial experiments, substances injected into SW 13 cells subjected only to propidium iodide labeling (see below) were supplemented with FITC-dextran (20,000 average molecular weight; Sigma) at 1 mg/ml to permit unequivocal identification of microinjected cells. For later experiments (i.e., those reported on in Figure 6 and Table 1), the dextran was omitted.

Cells, Microinjection, and Gel Electrophoresis

Primary human skin fibroblasts (HSF cells) (Höner *et al.*, 1991) and cells of the F8 subclone of the human adrenal cortex carcinoma cell line SW 13 (Beuttenmüller *et al.*, 1994) were cultured as previously described. The HSF cells possess vimentin IFs, whereas the SW 13 F8 cells are devoid of vimentin (or any other known cytoplasmic) IFs. Additional SW 13 cell lines (SW 13 [vimentin$^-$] and SW 13 T3 M [vimentin$^+$]) (Sarria *et al.*, 1990, 1992) were kindly provided by Dr. Robert Evans (University of Colorado Health Sciences Center, Denver, CO) and were grown as described. Cells for microinjection were grown on Eppendorf Cellocate coverslips (Eppendorf, Hamburg, Germany); the uninjected cells in surrounding quadrants of the coverslips served as additional controls. Microinjection was performed essentially as previously described (Höner *et al.*, 1991), except that some of the initial experiments were carried out with a Zeiss AIS automatic injection system (Zeiss, Oberkochen, Germany). Typically, ~20 (manual injection) to 100 or more (AIS injection) cells were injected for each test substance in each experiment. Syringe loading of HSF and SW 13 cells (5×10^5 cells) was performed as described (Clark and McNeil, 1992). Cells were incubated for 15–60 min (as indicated) at 37°C after microinjection or syringe loading, before further treatment for microscopy or gel electrophoresis. Where indicated, vimentin was introduced into SW 13 [vimentin$^-$] cells by microinjection of purified vimentin protein (2 mg/ml in 10 mM Na-phosphate, pH 7.0) 24 h before the injection of HIV-1 PR or the control bacterial extract. For some experiments, cells were permeabilized with either digitonin or Triton X-100 and the residual structures obtained were incubated with HIV-1 PR before analysis by gel electrophoresis, electron microscopy, or indirect immunofluorescence microscopy.

One- and two-dimensional gel electrophoresis was performed as described (Höner *et al.*, 1991) and according to the manufacturer's

Table 1. Statistical evaluation of the effect of microinjected substances on the distribution of chromatin in the nuclei of SW 13 [vimentin$^-$] cells

Substance injected	No. of cells analyzed	No. of cells with abnormal chromatin	Percent of cells with abnormal chromatin
MOPS buffer (10 mM, pH 7)	13	1	8
HIV-1 PR	10	0	0
Peptides derived from wild-type or deletion mutant vimentin proteins:			
NT1 peptide (residues 1–96)	18	16	89
1–51 peptide	12	12	100
1–60 peptide	10	10	100
1–92 peptide	11	10	91
423–465 peptide	10	0	0
17–51 peptide	11	1	9
17–60 peptide	12	12	100
17–92 peptide	11	10	91
32–51 peptide	11	2	18
32–60 peptide	12	0	0
32–92 peptide	12	11	92
1-Δ(25–38)-51 peptide	14	5	36
1-Δ(25–38)-60 peptide	17	16	94
1-Δ(25–38)-92 peptide	13	2	15
1-Δ(25–63)-92 peptide	16	0	0
1-Δ(25–68)-92 peptide	13	11	85
1-Δ(44–68)-92 peptide	14	12	86
Synthetic peptides identical to vimentin residues (as indicated in parentheses)			
R23R (22–44)	12	9	75
R25R (44–68)	16	9	56
P410 (3–22)	25	7	28
P411 (24–44)	25	19	76
P412 (83–103)	28	23	82

For these experiments, the HIV-1 PR (0.01 mg/ml) and the vimentin peptides (0.2 mM) were dissolved in 10mM MOPS, pH 7 buffer. In a control experiment, all SW 13 T3M [vimentin$^+$] cells injected with HIV-1 PR (13 of 13) exhibited nuclear aberrations. Cells were fixed 30 min after microinjection and stained with propidium iodide as described in MATERIALS AND METHODS. The indicated number of cells were evaluated by CLS microscopy. A single optical section, from the equatorial plane of the cell nucleus and characteristic of the entire series of sections, is presented for each substance injected in Figure 6.

instructions (Bio-Rad, Munich, Germany). Gels were scanned and analyzed with a Pharmacia Imagemaster DTS scanner and software (Amersham-Pharmacia Biotech, Braunschweig, Germany).

Antibodies

Polyclonal goat anti-vimentin antibody was affinity-purified against mouse vimentin, as previously described (Hartig *et al.*, 1997). A monoclonal mouse anti-human NuMA antibody was purchased from Serva (Heidelberg, Germany). Appropriate, FITC-labeled secondary antibodies were from either Sigma, Nordik (Tilburg, Holland), or Dakopatts (Glostrup, Denmark).

Other Materials

Bovine serum albumin, pepstatin A, pluronic F68, propidium iodide, 4′, 6-diamidino-2-phenylindole (DAPI), FITC-dextrans, and RNase A were purchased from Sigma. Antibed (diethyl diglycol distearate) was purchased from EM (Chestnut Hill, MA). Vectashield antifading agent was purchased from Serva. Other materials were reagent grade or as described in the references and were generally obtained from either Merck (Darmstadt, Germany), Pharmacia, Roth (Karlsruhe, Germany), or Sigma.

Preparation of Cells for Confocal Laser Scanning (CLS) Microscopy and Electron Microscopy

Cells were fixed in paraformaldehyde and glutaraldehyde, permeabilized with Triton X-100, and incubated with appropriate primary and secondary antibodies by using standard procedures. For CLS microscopy, the permeabilized cells were incubated in phosphate-buffered saline containing 10 U/ml RNase A for 60 min at 37°C and then mounted in embedding medium containing antifading agents and 2 μg/ml propidium iodide. Chromatin also was visualized with DAPI (Shoeman *et al.*, 1999) in cells stained with multiple antibodies for indirect immunofluorescence. Where indicated, some preparations were treated simultaneously with DAPI and RNase (using the same procedure as for propidium iodide staining of chromatin). Alternatively, for electron microscopy, resinless sections (Capco *et al.*, 1984; Fey *et al.*, 1986) were prepared from cells embedded in agarose, extracted with buffers CSK I and CSK II (with or without appropriate nuclease treatment to reveal the nuclear matrix), fixed in glutaraldehyde, dehydrated, and transferred to antibed. Sections of ~300-nm thickness were prepared for electron microscopy by using standard procedures. Antibed was extracted and the sections were critical point dried in CO_2. The sections were sputtered with tungsten at an angle of 5° and then coated with carbon. Sections

were viewed and photographed on a Zeiss EM902 electron microscope.

Confocal Laser Scanning Microscopy

CLS microscopy was initially performed on a Zeiss IM35 inverted microscope equipped with a Leica Lasertechnik CLS unit and an argon/krypton ion laser (Leica Lasertechnik, Heidelberg, Germany). Most images were produced using a 63× objective and were scanned using line averaging (8 or 16 scans/line) with an image Z plane spacing of 0.5 μm. For later experiments (Figures 5 and 6), a Leica TCS NT microscopy system with an argon/krypton laser, and an argon UV laser (Leica Microsystems Heidelberg GmbH, Heidelberg, Germany) was used. Images were obtained with either a 63 or 100× objective and were scanned using frame averaging (4 scans/frame) with an image Z plane spacing of 0.243 μm. Images were processed using Application Visualization System software from Advanced Video Systems (Waltham, MA) on a Silicon Graphics Indigo 2 workstation, as described (Hartig *et al.*, 1997). Where only one optical section is presented, it is the equatorial section from a serial section series and/or is representative of the entire series. In one case, pairs of images obtained from the red (propidium iodide) and green (FITC) channels are presented from the same series of optical sections in red and green pseudo colors. Figures were printed using Adobe Photoshop 5.02 software (Adobe Systems, San Jose, CA) and an HP 2000C inkjet printer (Hewlett Packard, Palo Alto, CA). Each experiment reported here was independently repeated two or more times, except for the data presented in Table 1 for which the statistics are provided; for Figures 1-5, the selected images in the figures are typical of the results observed with the entire series of cells treated. The data presented in Table 1 are summaries of the analysis of the entire series of sections obtained from >300 microinjected cells (5.9 gigabytes of data), with at least 10 cells analyzed for each peptide or treatment. Although necessarily subjective in nature, assignments as "normal" or "abnormal" were made by two independent observers and were conservative in nature (i.e., "intermediate" conditions were scored as positive for the MOPS buffer and as negative for the peptides). CLS microscopy parameters, such as photomultiplier gain and offset, pinhole diameter, and laser power, were held constant within any one experiment. Each set of data from each microscopy system was subjected to identical graphic analysis and printing.

RESULTS

Microinjection of the HIV-1 PR into fibroblast cells results in changes readily detectable at the light microscopic level, including alterations in nuclear shape and chromatin organization, dissolution of stress fibers, and a collapse of the vimentin IF network (Höner *et al.*, 1991; our unpublished results). Electron microscopy of resinless thick sections of HSF cells (Figure 1) after syringe loading revealed several HIV-1 PR-dependent effects. The most dramatic is a shift from a spherical or ovoid nuclear morphology in cells loaded with the control bacterial extract (Figure 1a) to one with multiple lobes or deep invaginations in cells loaded with the HIV-1 PR (Figure 1b). After syringe loading with the HIV-1 PR at a concentration of 35 μg/ml, the nuclear matrix collapsed, with individual elements noticeably thicker than in control-treated cells (Figure 1b), or, at a concentration of 70 μg/ml, was lost from the preparation such that only peripheral rudiments remained (Figure 1c). The extreme nuclear periphery, corresponding to the region where the nuclear lamina and tightly bound chromatin are expected to be associated with the nuclear envelope, generally contained more electron dense material and was generally thicker in cross section in the HIV-1 PR-treated cells (L in Figure 1e) relative to control bacterial extract-treated cells (L in Figure 1d). The changes in nuclear shape and chromatin organization also were clearly detectable using CLS microscopy of propidium iodide-stained, microinjected cells. In contrast to the relatively uniform staining of nuclear chromatin seen in optical sections of HSF cells microinjected with control bacterial extract (Figure 2A), wholesale condensation of chromatin and multiple nuclear membrane invaginations were visible in cells microinjected with HIV-1 PR (Figure 2B). Because the morphology of the control and HIV-1 PR-treated nuclei of the HSF cells observed in CSL microscopy was so similar to that observed in electron microscopy, further microscopic investigations were performed using CSL microscopy. It should be noted that the effects on nuclear chromatin organization readily visible in the propidium iodide-stained cells (Figure 2) were not apparent when similarly treated cells were stained with DAPI by using the standard protocol. Inclusion of a RNase treatment step in the DAPI staining protocol yielded results similar to those seen with propidium iodide staining (our unpublished results).

Although the cleavage of vimentin was readily detectable in these cells, our attempts to identify a major nuclear structural protein (via 1D- and 2D-gel electrophoresis) whose cleavage by the HIV-1 PR might be responsible for these alterations in nuclear architecture have, to date, been unsuccessful (our unpublished results). The nuclear lamin A, B, and C proteins were not detectably cleaved (our unpublished results). We have previously reported preliminary results (Shoeman *et al.*, 1996) and hereby confirm that NuMA is cleaved by treatment with HIV-1 PR (our unpublished results); however, the cleavage of NuMA proved to be a surrogate marker for, rather than the cause of, the nuclear alterations. Detailed analysis of the effect of the HIV-1 PR on nuclear organization were hampered not only by a lack of antibodies or other reagents reacting specifically with the core filaments of the nuclear matrix but also by the fact that these structures were unaffected by direct treatment of either digitonin- or Triton X-100-permeabilized cells with HIV-1 PR (our unpublished results). As in previous experiments (Höner *et al.*, 1991), extensive cleavage of vimentin was consistently observed (our unpublished results). We therefore chose to investigate whether the cleavage of vimentin was correlated with any of the nuclear alterations observed in these cells.

Changes in nuclear architecture and chromatin distribution were observed in SW 13 T3 M [vimentin$^+$] cells after microinjection of HIV-1 PR (Figure 3C), compared with cells injected with control solution (Figure 3A), although the changes in nuclear shape were less dramatic than those observed with the HSF cells, in part due to the more irregular shape of the nuclei in SW 13 cells compared with HSF cells. No reproducible nuclear changes were observed in any of the SW 13 [vimentin$^-$] cells (regardless of origin) after treatment with HIV-1 PR (Figure 3D) or bacterial control extract (Figure 3B), either after microinjection (Figure 3) or syringe loading (our unpublished results).

A second type of experiment was performed to confirm whether the presence of vimentin plays a role in the HIV-1 PR-mediated nuclear changes. This approach involved the microinjection of vimentin, before the microinjection of the

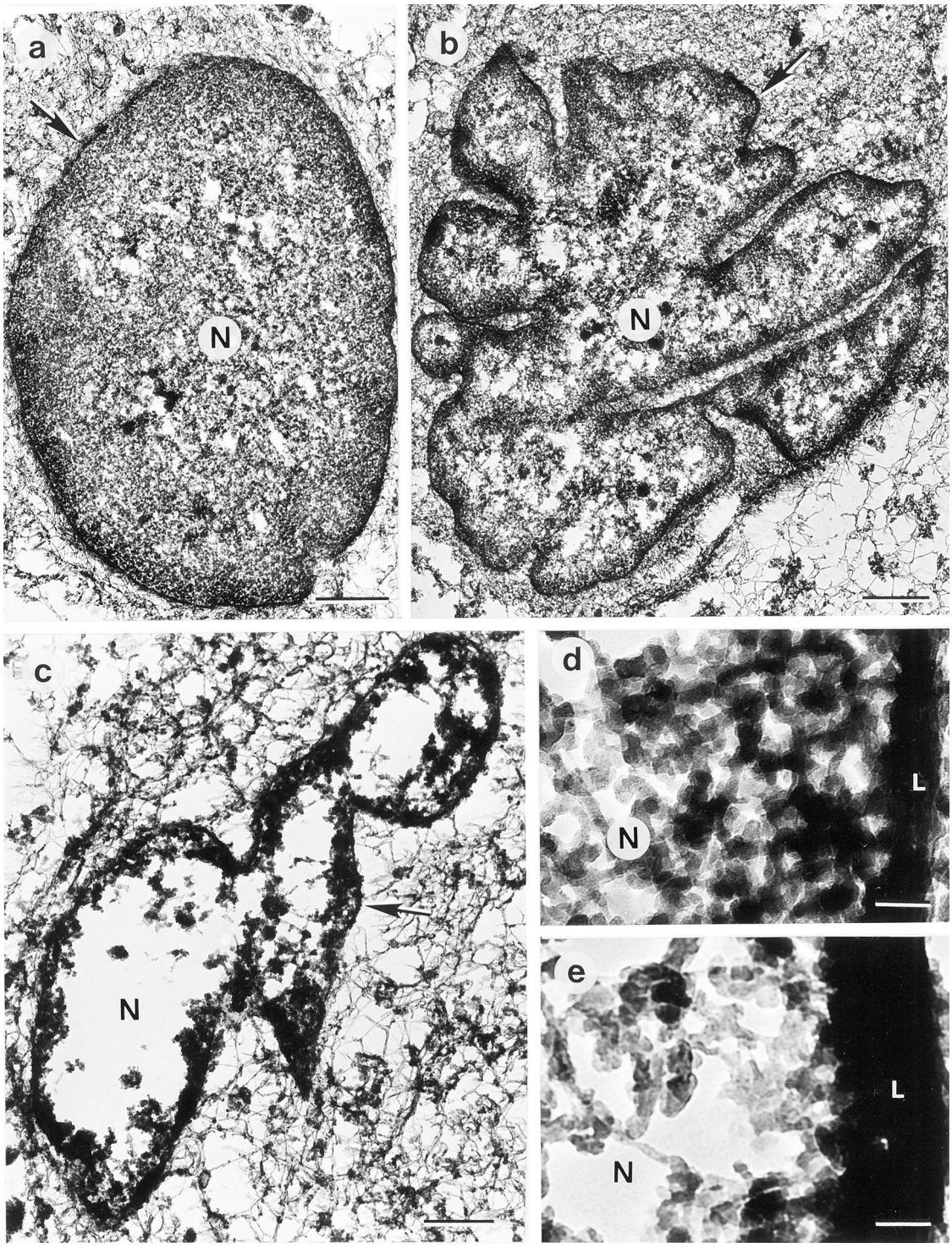

Figure 1. Resinless thick sections of HSF cells syringe-loaded with control bacterial extract (a and d) or HIV-1 PR at 35 μg/ml (b and e) or 70 μg/ml (c). The cells were incubated for 30 min at 37°C after syringe loading, embedded in agarose, and prepared for electron microscopy as described in MATERIALS AND METHODS. In cells treated with the control bacterial extract (a and d), the nucleus (N) is uniformly spherical or ovoid, possesses a well-defined nuclear lamina (arrow in a–c, white letter L in d and e) and is filled with an extensive and dense matrix of fibers and filaments. In cells treated with HIV-1 PR, the nuclear periphery is lobed and invaginated (b) and becomes considerably thicker than in control cells (compare L in d and e). In cells subjected to more extensive treatment with HIV-1 PR (c), the nuclear matrix is lost and the nuclear periphery becomes even more prominent, presumably due to the collapse of nuclear matrix remnants onto the lamina. Bar, 1 μm (a–c); 0.1 μm (d and e).

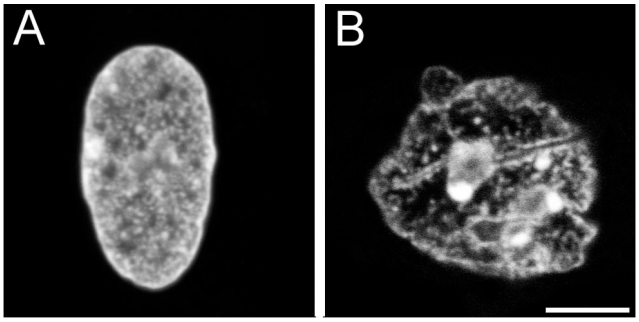

Figure 2. Distribution of nuclear chromatin in HSF cells injected with either control bacterial extract (A) or HIV-1 PR (B). After microinjection, the cells were incubated for 15 min at 37°C and fixed; DNA was stained with propidium iodide and the preparations were subjected to CLS microscopy. Note the wholesale condensation of chromatin and multiple nuclear membrane invaginations in the HIV-1 PR-injected cell, similar to that seen in the electron micrographs of syringe-loaded fibroblasts (Figure 1, b and c). Bar, 10 μm.

HIV-PR or vimentin peptides into SW 13 [vimentin$^-$] cells. Preinjection of vimentin into SW 13 [vimentin$^-$] cells led to the formation of a cytoplasmically extended IF network surrounding the nucleus, both of which were not changed in their organization and structure after microinjection of control bacterial extract (our unpublished results). However, microinjection of HIV-1 PR into such cells brought about substantial alterations in the structure of the vimentin IF network and in nuclear chromatin staining and distribution (our unpublished results). Nuclear shape was not affected. The same changes in nuclear chromatin staining and distribution were observed in SW 13 [vimentin$^-$] cells after the injection of a mixture of vimentin peptides, produced by the cleavage of vimentin to completion by the HIV-1 PR in vitro (Figure 4B), whereas these effects could not be seen in control SW 13 [vimentin$^-$] cells microinjected with HIV-1 PR (Figure 4A). As illustrated in Figure 4C, even the isolated amino-terminal peptide of vimentin, NT1, was able to induce structural changes in the nuclei of SW 13 [vimentin$^-$] cells. Microinjection of the vimentin NT1 peptide into SW 13 T3 M [vimentin$^+$] cells resulted in condensation of chromatin and alterations in nuclear shape (Figure 4D), as well as in a perturbation of the endogenous vimentin IF network (our unpublished results). In control experiments (Figure 5), F-cys$_1$-NT1 (*m/z* 10,705) was found in both the cytoplasm and nucleus after microinjection into SW 13 [vimentin$^-$] cells (Figure 5A). Likewise, both a vimentin$_{1-104}$ NT-GFP (green fluorescent protein) fusion protein (M_r ~38,000) and native GFP were found in both the cytoplasm and nucleus of transiently transfected cells (our unpublished results). T-vimentin remained in the cytoplasm of injected cells and had no effect on chromatin distribution (Figure 5B). FITC-dextran, 70,000 MW, remained in the cytoplasm and had no effect on chromatin distribution (Figure 5C), whereas FITC-dextran, 4000 MW, was found in both the cytoplasm and nucleus and likewise had no effect on chromatin distribution (our unpublished results).

The results presented in the first five figures are typical results from the evaluation of >150 individual cells. To get a more statistically significant overview and to delineate

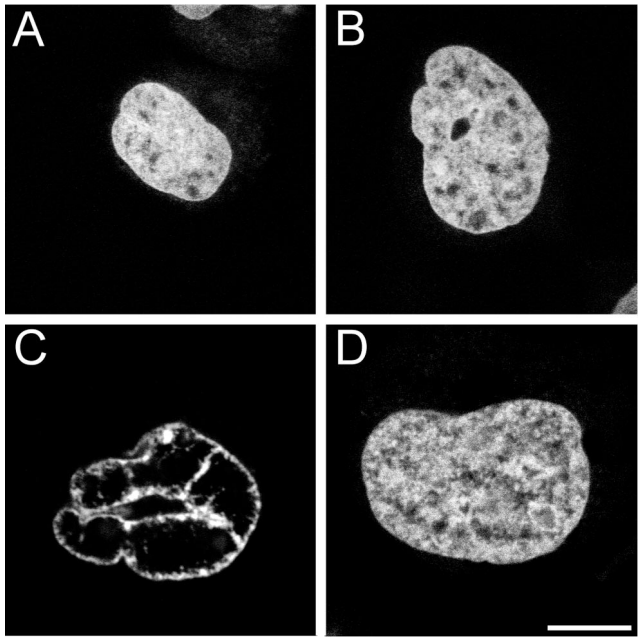

Figure 3. Presence of the cytoplasmic IF protein vimentin correlates with the occurrence of nuclear aberrations in SW 13 cells after microinjection of the HIV-1 PR. After microinjection of either SW 13 T3 M [vimentin$^+$] cells (A and C) or SW 13 [vimentin$^-$] cells (B and D), the cells were incubated for 30 min at 37°C and fixed; DNA was stained with propidium iodide and the preparations were examined via CLS microscopy. (A and B) Distribution of chromatin in the cells of the cell lines SW 13 T3 M [vimentin$^+$] and SW 13 [vimentin$^-$], respectively, after microinjection with control bacterial extract control buffer. Equatorial optical sections of the chromatin distribution of a SW 13 T3 M [vimentin$^+$] cell (C) and of a SW 13 [vimentin$^-$] cell (D) after microinjection with HIV-1 PR are presented. Although the effect of the action of HIV-1 PR on nuclear chromatin organization is dramatic, the effect on nuclear shape is less obvious, partially due to the more irregular shape of the nuclei of SW 13 cells in comparison to fibroblasts. Bar, 10 μm.

those residues of the vimentin peptides responsible for the effects observed, a large number of SW 13 [vimentin$^-$] cells were microinjected with various purified peptides, each at a final concentration of 0.2 mM, or control substances and subjected to CLS microscopy and analysis. A panel of typical images obtained in this study is presented in Figure 6 and the tabulated data for the 346 cells analyzed is presented in Table 1. The nuclei of cells injected with buffer (Figure 6A and Table 1) were not detectably different from uninjected controls. Microinjection of the carboxy-terminal peptide released from the primary cleavage of vimentin by HIV-1 PR (Shoeman *et al.*, 1990a), vimentin$_{423-465}$, had no effect on chromatin (Figure 6H and Table 1). All three amino-terminal peptides, produced by the secondary cleavage of vimentin (Shoeman *et al.*, 1990a), vimentin$_{1-51}$, vimentin$_{1-60}$, and vimentin$_{1-92}$, each individually affected chromatin distribution in SW 13 [vimentin$^-$] cells (Figure 6, E–G, and Table 1) as efficiently as the mixture produced by action of the HIV-1 PR on vimentin (Figure 4). Internal peptides, vimentin$_{17-60}$ and vimentin$_{17-92}$, produced from the vimentin Δ17 mutant protein, also affected chromatin distribution in SW 13 [vi-

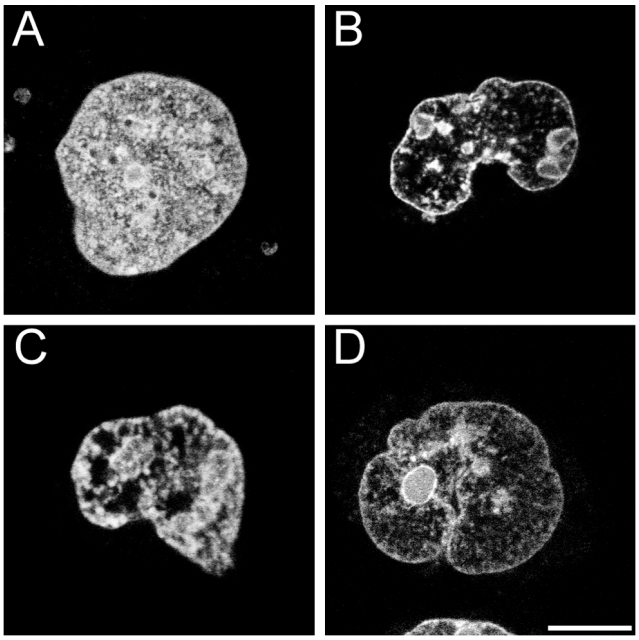

Figure 4. Microinjection of the mixture of vimentin cleavage products produced in vitro by the action of HIV-1 PR or a defined vimentin peptide encompassing the entire amino-terminal head domain into SW 13 [vimentin$^-$] cells also produces nuclear chromatin condensation and redistribution, but has no effect on nuclear shape. CLS microscopy optical sections of the chromatin distribution of a cell microinjected with HIV-1 PR (7 μg/ml) as a control (A) and a cell microinjected with a mixture of vimentin cleavage products (produced from overnight digestion of vimentin at 0.2 mg/ml) (B) demonstrate that the vimentin peptides, and not the HIV-1 PR, are directly responsible for the nuclear effects. Microinjection of the isolated amino-terminal peptide of mouse vimentin, NT 1 (vimentin residues 1–96), into SW 13 [vimentin$^-$] cells resulted in nuclear alterations (C), similar to those seen with the vimentin cleavage product mixture or in SW 13 T3 M [vimentin$^+$] cells injected with HIV-1 PR (Figure 2). Microinjection of NT 1 into SW 13 T3 M [vimentin$^+$] cells and incubation for 30 min at 37°C also resulted in condensation of chromatin and alteration in nuclear shape (D) and a perturbation of the vimentin IF network (our unpublished results). Injected cells were incubated for 30 min at 37°C before fixation, staining with propidium iodide and preparation for CLS microscopy. Bar, 10 μm (A–D).

mentin$^-$] cells (Figure 6, J and K, and Table 1). The results obtained with the other deletion peptides and the smaller synthetic peptides were somewhat more complicated (Figure 6 and Table 1). Two different regions appear equally able to elicit chromatin aberrations: one region corresponds to part or all of the two DNA-binding wings of vimentin (residues 27–62) and another distal to that (within residues 68–92). Although restraint should be exercised to avoid overinterpreting the data obtained with the mutant peptides (which do not normally occur in nature), it appears as if the first 25 amino acid residues may, in combination with the deletion of the middle of the head domain, inhibit the ability of the distal region to affect chromatin organization, perhaps by interacting with residues between amino acids 63 and 68 (compare the activities of the 1-Δ(25–63)-92 and 1-Δ(25–68)-92 peptides; Table 1). HIV-1 PR had no effect on chromatin in SW 13 [vimentin$^-$] cells (Figure 6B and Table 1), but had a dramatic effect on chromatin organization in SW 13 T3 M [vimentin$^+$] cells (Figure 6C and Table 1). Together, these results suggest that residues in two regions of the vimentin head domain, i.e., vimentin$_{17-60}$ and vimentin$_{68-92}$, are those primarily responsible for the effects observed on chromatin organization.

DISCUSSION

HIV-1 PR introduced into HSF cells results in dramatic changes in nuclear shape and organization, as well as in alterations of the cytoskeleton, which have been described at the level of conventional light microscopy (Shoeman *et al.*, 1990a, 1993; Höner *et al.*, 1991). Although many mammalian cells are known to contain deep tubular invaginations of the nuclear envelope (Fricker *et al.*, 1997), some of which are associated with perinuclear rings of IFs (Kamei, 1994), and nuclei of the cell line SW 13 are generally irregular in shape (Sarria *et al.*, 1994), the invaginations described in this article in HSF and SW 13 T3 M [vimentin$^+$] cells correlate with treatment with the HIV-1 PR. Given the propensity for HIV-1 PR to cleave IF proteins (Shoeman *et al.*, 1990a), we had originally thought that the nuclear matrix core filaments, which are morphologically indistinguishable from the cytoplasmic IFs (Jackson and Cook, 1988; He *et al.*, 1990; Wang and Traub, 1991; Padros *et al.*, 1997), or other compo-

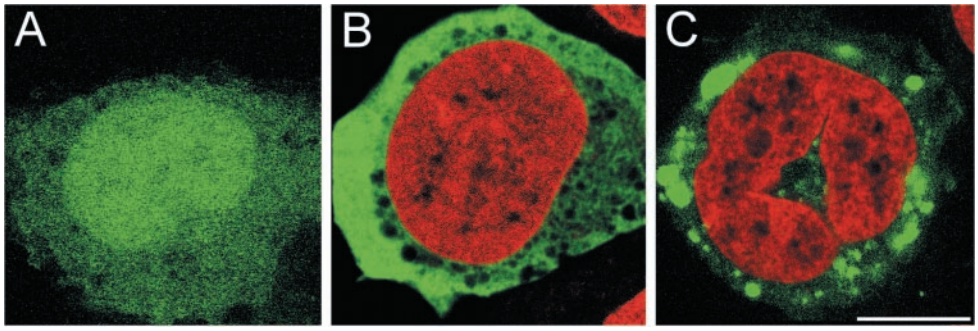

Figure 5. Intracellular distribution of vimentin peptides and control substances after microinjection into SW 13 [vimentin$^-$] cells. F-cys$_1$-NT1 is found in both the cytoplasm and nucleus (A, fluorescein channel). T-vimentin (B, composite panel of both fluorescein channel [green] and propidium iodide channel [red]), visualized with an anti-vimentin antibody and an FITC-labeled second antibody, remains in the cytoplasm (fluorescein channel) and has no effect on nuclear structure or chromatin distribution (propidium iodide channel). FITC-dextrans of molecular weight 20–70,000 or higher remained in the cytoplasm and had no effect on nuclear architecture (C, composite of both fluorescein channel [green] and propidium iodide channel [red] after microinjection of MW 70,000 FITC-dextran). Smaller dextrans (i.e., MW 4000 FITC-dextran) were distributed throughout the cell, i.e., readily entered the nucleus, but had no effect on nuclear architecture (our unpublished results). Bar, 10 μm (A–C).

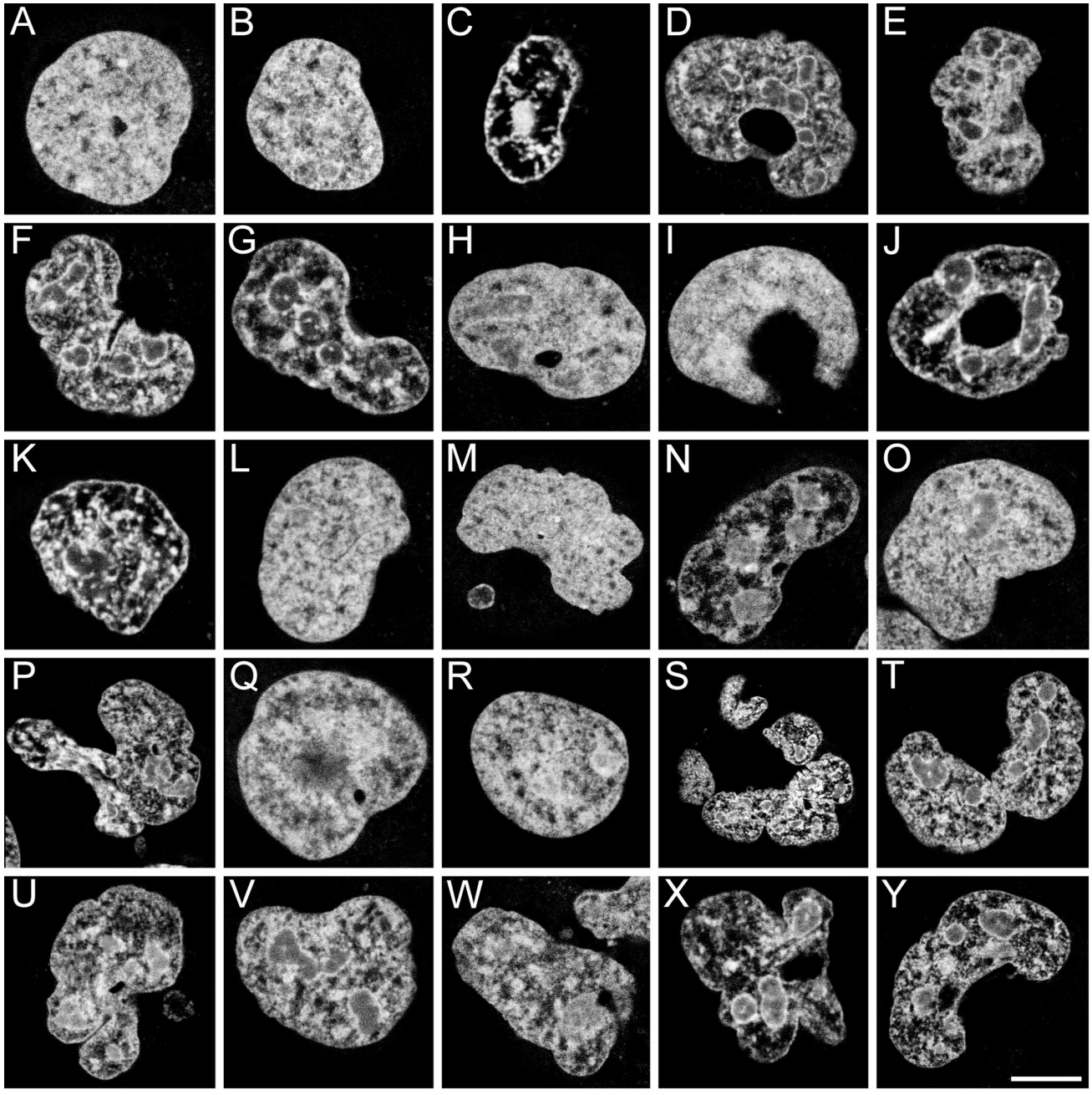

Figure 6. Typical optical sections of cells microinjected with the peptides and substances listed in Table 1. All peptides were used at a concentration of 0.2 mM in 10 mM MOPS, pH 7. All panels show SW 13 [vimentin$^-$] cells, except for C in which a SW 13 T3 M [vimentin$^+$] cell is shown. Substances injected were MOPS buffer (A); HIV-1 PR, 10 μg/ml in 10 mM MOPS, pH 7 (B); HIV-1 PR, 10 μg/ml in 10 mM MOPS, pH 7, microinjected into an SW 13 T3 M [vimentin$^+$] cell (C); vimentin peptide NT1 (vimentin$_{1-96}$) (D); vimentin$_{1-51}$ (E); vimentin$_{1-60}$ (F); vimentin$_{1-92}$ (G); vimentin$_{423-465}$ (H); vimentin$_{17-51}$ (I); vimentin$_{17-60}$ (J); vimentin$_{17-92}$ (K); vimentin$_{32-51}$ (L); vimentin$_{32-60}$ (M); vimentin$_{32-92}$ (N); vimentin$_{1-\Delta(25-38)-51}$ (O); vimentin$_{1-\Delta(25-38)-60}$ (P); vimentin$_{1-\Delta(25-38)-92}$ (Q); vimentin$_{1-\Delta(25-63)-92}$ (R); vimentin$_{1-\Delta(25-68)-92}$ (S); vimentin$_{1-\Delta(44-68)-92}$ (T); peptide R23R (vimentin$_{22-44}$) (U); peptide R25R (vimentin$_{44-68}$) (V); peptide P410 (vimentin$_{3-22}$) (W); peptide P411 (vimentin$_{24-44}$) (X); and peptide P412 (vimentin$_{83-103}$) (Y). Bar, 10 μm (A–Y).

nents of the nuclear matrix, such as the intranuclear matrix protein, which is related to the nuclear lamins (Menz *et al.*, 1996), would be extensively cleaved by HIV-1 PR. This could not be shown so far. Results of experiments not presented here have shown that these intranuclear filament systems are unaffected by treatment of detergent-permeabilized cells with HIV-1 PR. Although the NuMA protein is cleaved by HIV-1 PR, the facts that the HIV-1 PR treatment of SW 13

[vimentin$^-$] cells (whose nuclei contain NuMA) has no influence on nuclear organization, whereas microinjection of vimentin peptides does, demonstrate that the cleavage of NuMA (or any other as-yet-unidentified nuclear component) occurs incidental to the events that ultimately perturb nuclear architecture.

Comparison of results obtained after microinjection of HIV-1 PR into SW 13 [vimentin$^-$] and SW 13 T3 M [vimentin$^+$] cells or into SW 13 [vimentin$^-$] cells previously injected with vimentin provided the first indication that the cleavage products of vimentin might be the effector molecules responsible for the changes in nuclear organization. This was largely substantiated by the microinjection of a mixture of vimentin peptides (produced by limit digestion with HIV-1 PR) into SW 13 [vimentin$^-$] cells: alterations in chromatin distribution and condensation were seen, but nuclear morphology was unaffected. Critically important to the interpretation and conclusions of this study are the data obtained from control experiments: the organization of the nuclei of cells lacking vimentin remains unaffected by treatment with HIV-1 PR. Because the limit digest of vimentin by HIV-1 PR produces a mixture of several peptides (Shoeman *et al.*, 1990a,b), corresponding roughly to the head domain, the rod domain and the tail domain, and because it has been shown that the various domains of vimentin can interact with themselves and some other related proteins (Traub *et al.*, 1992b; Meng *et al.*, 1996) as well as with histones (Traub *et al.*, 1986), it was of interest to define which peptide(s) of this mixture was responsible for the changes observed. The amino-terminal peptide NT1 was originally chosen because it was available in sufficient quantity and purity, is almost identical to the largest amino-terminal peptide produced by HIV-1 PR, and because it encompasses a domain of vimentin known to be involved in interactions with a variety of compounds, including nucleic acids, lipids, and coiled-coil protein structures (Traub *et al.*, 1992b and references therein). Changes in chromatin distribution were seen after microinjection of NT1 into SW 13 [vimentin$^-$] cells. The changes were identical to those produced by microinjection of the HIV-1 PR-vimentin cleavage products. However, other peptides are also produced (Shoeman *et al.*, 1990a). Therefore, the 16 vimentin peptides liberated after HIV-PR treatment of wild-type and deletion mutant vimentin (Table 1) were all purified by HPLC and identified by their masses in MALDI-TOF analysis. Interestingly, only peptides derived from the N-terminal head domain of vimentin had an effect on nuclear architecture (Figure 6). F-cys$_1$-NT1 alone, or as a fusion protein with green fluorescent protein, was found both in the cytoplasm and in the nucleus of microinjected or transfected cells. Because all of the other peptides tested (Table 1) are smaller than NT1 (*m/z* values range from 2041 to 9739; NT1 is *m/z* 10,283), it is likely that they, too, can enter the nucleus unimpeded by the nuclear pores. Larger vimentin peptides, such as T-vimentin did not enter the nucleus and, importantly, had no effect on nuclear architecture. If the site of action of these peptides is cytoplasmic (i.e., the nuclear effect is an indirect one), it might be expected that T-vimentin should have had an effect on nuclear chromatin organization (because it possesses residues 71–103 of the head domain and thus has at least one of the active domains [see Table 1, peptide 412, vimentin$_{83–103}$]). Because it did not, it is likely that the effect of the vimentin peptides is exerted within the nucleus directly on the nuclear matrix or chromatin itself. Taken together, these results suggest that the head domain of vimentin alone is sufficient to perturb chromatin organization in vivo and, furthermore, that the head domain must be liberated from the IF to exert this activity. At least some of the effect of vimentin peptides may be a result of direct interaction of these peptides with nuclear DNA: the DNA binding domain of vimentin has been localized to the middle of the head domain (Shoeman *et al.*, 1999) and, in fact, tyrosine residues Y_{29}, Y_{37}, and Y_{52} can be photo-cross-linked to DNA bound to vimentin (Wang *et al.*, 2000). The amino-terminal polypeptides of vimentin also may interact with and perturb the 10-nm filament network of the nucleus, thus directly causing the changes in chromatin organization observed. Alternatively, the head domain of vimentin may function as a competitive inhibitor for the lamin B receptor and/or the nuclear lamina, both of which probably provide binding sites for chromatin at the nuclear envelope/periphery (Höger *et al.*, 1991; Luderus *et al.*, 1994; Pyrpasopoulou *et al.*, 1996). Disturbance of nuclear lamina organization by a dominant negative mutant lamin protein has been shown to affect the distribution of several replication factors and to inhibit DNA synthesis (Spann *et al.*, 1997).

It is intriguing that only changes in chromatin distribution but no reproducible alterations in nuclear shape were detected in SW 13 [vimentin$^-$] cells, regardless of the peptides injected. On the other hand, alterations in both chromatin organization and nuclear shape, as well as perturbations in the cytoplasmic vimentin IF network, were observed in SW 13 T3 M [vimentin$^+$] cells after microinjection not only of HIV-1 PR but also of NT1. Sarria *et al.* (1994) have previously shown that the nuclei of SW 13 cells are more smooth and regular in appearance when an intact vimentin IF network is present and, furthermore, that disruption of the vimentin IF network by coexpression of a truncated vimentin in these cells gives rise to major alterations in nuclear shape. The conclusion that can be made from these results based on the two disparate approaches is that, when present, an intact vimentin IF cytoplasmic network plays an important role in the establishment and maintenance of a regular nuclear morphology. Because no effect on nuclear shape was observed in SW 13 [vimentin$^-$] cells, preinjected with vimentin before the injection of HIV-1 PR, it may be possible that the IFs, when present, must engage in temporally or spatially specific interactions with the nucleus before an effect can be observed.

In a more global sense, electron microscopy of whole-mount preparations has revealed a continuum of filaments, extending from the outside of the cell to the interior of the nucleus (French *et al.*, 1989; Carmo-Fonseca and David-Ferreira, 1990). Maniotis *et al.* (1997) have shown that this continuum exists in living cells and that IFs play an important role in the transduction of mechanical signals from the extracellular matrix to the nuclear interior. These data provide support for models of gene regulation (Lelievre *et al.*, 1996; Ingber, 1997) that postulate physical connections between the surface of cells and the nucleus, disruption of which may play a role in transformation and carcinogenesis. The methods and reagents used in this study lend themselves to more detailed investigations in this direction and in the general field of chromatin and nuclear matrix interactions and organization. It will be of interest to identify the

target(s) with which the vimentin peptides interact; hopefully, such information might provide insight into the normal arrangement of chromatin and the nuclear matrix. Because the head domain peptides of vimentin do not contain any free amino groups, it was not possible to label them with amine reactive reagents or to fix these peptides with aldehydes for localization via indirect immunofluorescence. If problems of poor immunogenicity and fixation can be successfully addressed (perhaps by site-directed mutagenesis), immunoelectron microscopy might prove suitable to localize the vimentin peptides in treated cells and thus provide an explanation for how the changes in nuclear organization are brought about. The results of experiments designed to localize the amino terminal peptides in microinjected cells were particularly disappointing due to their ambiguity: NT1-GFP fusion protein was found in the nucleus, but showed no ability to perturb chromatin and, furthermore, GFP alone also was found in the nucleus.

What is the relevance of these observations with respect to infection by HIV-1 and other related retroviruses? Vimentin may participate in the uptake of HIV-1 preintegration complexes into the nuclear compartment (Thomas *et al.*, 1996) and appears to be important for the cytoplasmic localization of the HIV-1 Vif protein, which regulates viral infectivity by controlling either virus maturation and/or interaction with the cytoskeleton after virus entry (Karczewski and Strebel, 1996). It has been shown that vimentin is cleaved in vivo by the HIV-1 PR after microinjection (Höner *et al.*, 1991), as well as within HIV-1-infected cells (Lindhofer *et al.*, 1993; Konvalinka *et al.*, 1995). A genetic dimer of HIV-1 PR is active when expressed in host cells and exerts a cytopathic or toxic effect (Kräusslich, 1991). Up to 50% of the HIV-1 PR activity of cytopathic strains of HIV-1 is not associated with virions and gives rise to inappropriate processing of the viral polyproteins (Kaplan and Swanstrom, 1991); presumably, susceptible cellular proteins also are cleaved under these conditions, although this was not addressed in this study. In this respect, it is well known that HIV-1 (and many other retroviruses) is not very efficient in terms of packaging viral proteins into intact virions (Brown *et al.*, 1996). HIV-1 PR plays a crucial role in the early phase of viral replication (Nagy *et al.*, 1994) because PR inhibitors effectively block viral replication in a single cycle of infection, altering the stability of unintegrated viral cDNA and affecting the proper formation of the preintegration complex and/or its transport to the nucleus.

We have previously proposed that the HIV-1 PR may play a direct role in cytopathogenesis associated with infection by HIV-1 (Shoeman *et al.*, 1992, 1993). Although HIV-1 cytopathogenesis is most often correlated with syncytia formation, it is noteworthy that treatment of HIV-1-infected macrophage cultures in vitro with a PR inhibitor abolished cytopathogenesis but not syncytia formation (Bergamini *et al.*, 1996). It is unclear how much (or how little) PR activity is actually present in HIV-1-infected cells. Apparently, a lower threshold exists (Rosé *et al.*, 1995), below which mutations in viral polyprotein cleavage sites are selected for to compensate for the lowered PR activity of the mutant PRs expressed when HIV-1 strains are serially passaged in the presence of PR inhibitors (Croteau *et al.*, 1997). It will be of interest to see whether such mutant PRs also show reduced cleavage of cellular protein substrates and thus reduced contributions to cytopathogenesis. In HIV-1-infected individuals, condensation or degeneration of nuclear chromatin has been described in cells from a variety of tissues (Shoeman *et al.*, 1992, 1993 for references and discussion). Furthermore, complications of infection with HIV-1 include an unexplained increase in incidence of cancer, particularly lymphomas. Attempts at identifying an additional agent responsible for non-Hodgkin's lymphoma in a large HIV-1-infected cohort have failed (Armenian *et al.*, 1996), raising the possibility that HIV-1 itself is directly responsible. We have previously described a model that proposes a role for vimentin (and other IF subunit proteins) in the global regulation of gene expression (Traub and Shoeman, 1994). If this model is correct, then the ability of the HIV-1 PR to liberate amino-terminal peptides from vimentin provides a direct means for HIV-1 to interfere with host cell gene expression. Although it is not possible to "prove" that the cleavage of vimentin by HIV-1 PR makes "sense," there is no doubt that it occurs: indeed, native vimentin is one of the best substrates for HIV-1 PR (Shoeman *et al.*, 1990a) and it contains cleavage sites that fit theoretical models very well (Chou *et al.*, 1996). The liberation of the head domain of vimentin by HIV-1 PR may be an important aspect of the HIV-1 replication cycle because it perturbs IF organization and the ability of IFs to interact with important viral proteins or events (Thomas *et al.*, 1996). An added consequence of this cleavage would be the perturbation of nuclear chromatin organization by the vimentin head domain peptides. These changes may be more subtle and long term in affected cells of HIV-1-infected individuals because the total amount of active HIV-1 PR per cell (but not the concentration in areas of viral entry or budding; see Shoeman *et al.*, 1990b) is probably lower than that used in these cell biology experiments. This proposal is supported by our previous study in which we found changes in nuclear chromatin organization at levels of HIV-1 PR activity that were not sufficient to cause detectable changes in the vimentin IF network (Höner *et al.*, 1991); the amino-terminal peptides of vimentin affect nuclear architecture, and presumably nuclear function, long before the organization of the cytoplasmic IF network is disturbed. It is now clear that this apparently paradoxical situation is due to the exquisite sensitivity of the nuclear events and the relative resistance of the IF network to the presence of the vimentin head domain peptides. The collapse of the IF network after the removal of the terminal domains by action of the HIV-1 PR would be expected to be a "late" event in these experiments because it has been shown that the fraction of N-terminally truncated vimentin molecules that can be tolerated in a normal IF network is ~25% (Andreoli and Trevor, 1994). In light of the results presented in this article and the ability of HIV-1 PR to degrade myofibrils when applied exogenously (Shoeman *et al.*, 1993), it becomes especially important to consider treating HIV-1-infected individuals with HIV-1 PR inhibitors to not only block viral replication but to also prevent the HIV-1 PR from contributing to cytopathogenesis and carcinogenesis.

ACKNOWLEDGMENTS

Some of these studies were part of a doctoral thesis presented by C.H. in partial fulfillment for the requirements of a Ph.D. program

at the Ruhr University of Bochum, Bochum, Germany. We thank Margot Bialdiga (deceased), Annemarie Scherbarth, and Ulrike Traub for providing tissue culture cells; Annegret Gawenda for assistance with photography; Qiang Wang for performing the HPLC purification of the vimentin peptides; Dr. Ulrike Niesel for performing the experiments with the vimentin$_{1-104}$ NT-GFP fusion protein; and Dr. Günter Giese for initial assistance with CLS microscopy and graphic analysis.

REFERENCES

Andreoli, J.M., and Trevor, K.T. (1994). Fate of a headless vimentin protein in stable cell cultures: soluble and cytoskeletal forms. Exp. Cell Res. *214*, 177–188.

Armenian, H.K., Hoover, D.R., Rubb, S., Metz, S., Martinez-Maza, O., Chmiel, J., Kingsley, L., and Saah, A. (1996). Risk factors for non-Hodgkin's lymphomas in acquired immunodeficiency syndrome (AIDS). Am. J. Epidemiol. *143*, 374–379.

Bergamini, A., Dini, L., Capozzi, M., Ghibelli, L., Placido, R., Faggioli, E., Salanitro, A., Buonanno, E., Cappannoli, L., Ventura, L., Cepparulo, M., Falasca, L., and Rocchi, G. (1996). Human immunodeficiency virus-induced cell death in cytokine-treated macrophages can be prevented by compounds that inhibit late stages of viral replication. J. Infect. Dis. *173*, 1367–1378.

Beuttenmüller, M., Chen, M., Janetzko, A., Kühn, S., and Traub, P. (1994). Structural elements of the amino-terminal head domain of vimentin essential for intermediate filament formation *in vivo* and *in vitro*. Exp. Cell Res. *213*, 128–142.

Brown, A.E., Vahey, M.T., Zhou, S.Y.J., Chung, R.C.Y., Ruiz, N.M., Hofheinz, D., Lane, J.R., Mayers, D.L., Hawkes, C.A., and Malone, J.L. (1996). Relationship between immune complex-dissociated p24 antigen and human-immunodeficiency-virus type-1 RNA titers in plasma-reply. J. Infect. Dis. *173*, 1523–1524.

Capco, D.G., Krockmalnic, G., and Penman, S. (1984). A new method of preparing embedment-free sections for transmission electron microscopy: applications to the cytoskeletal framework and other three-dimensional networks. J. Cell Biol. *98*, 1878–1885.

Carmo-Fonseca, M., and David-Ferreira, J.F. (1990). Interactions of intermediate filaments with cell structures. Electron Microsc. Rev. *3*, 115–141.

Chou, K-C., Tomasselli, A.G., Reardon, I.M., and Heinrikson, R.L. (1996). Predicting human immunodeficiency virus protease cleavage sites in proteins by a discriminant function method. Proteins Struct. Funct. Genet. *24*, 51–72.

Clark, M.S., and McNeil, P.L. (1992). Syringe loading introduces macromolecules into living mammalian cell cytosol. J. Cell Sci. *102*, 533–541.

Croteau, G., Doyon, L., Thibeault, D., McKercher, G., Pilote, L., and Lamarre, D. (1997). Impaired fitness of human immunodeficiency virus type 1 variants with high-level resistance to protease inhibitors. J. Virol. *71*, 1089–1096.

Fey, E.G., Krockmalnic, G., and Penman, S. (1986). The non-chromatin substructures of the nucleus: the ribonucleoprotein (RNP)-containing and RNP-depleted matrices analyzed by sequential fractionation and resinless section electron microscopy. J. Cell Biol. *102*, 1654–1665.

French, S.W., Kawahara, H., Katsuma, Y., Ohta, M., and Swierenga, S.H.H. (1989). Interaction of intermediate filaments with nuclear lamina and cell periphery. Electron Microsc. Rev. *2*, 17–51.

Fricker, M., Hollinshead, M., White, N., and Vaux, D. (1997). Interphase nuclei of many mammalian cell types contain deep, dynamic, tubular membrane-bound invaginations of the nuclear envelope. J. Cell Biol. *136*, 531–544.

Graves, M.C., Lim, J.J., Heimer, E.P., and Kramer, R. (1988). An 11-kDa form of human immunodeficiency virus protease expressed in *Escherichia coli* is sufficient for enzymatic activity. Proc. Natl. Acad. Sci. USA *85*, 2449–2453.

Hartig, R., Huang, Y., Janetzko, A., Shoeman, R., Grüb, S., and Traub, P. (1997). Binding of fluorescence- and gold-labeled oligodeoxyribonucleotides to cytoplasmic intermediate filaments in epithelial and fibroblast cells. Exp. Cell Res. *233*, 169–186.

He, D., Nickerson, J.A., and Penman, S. (1990). Core filaments of the nuclear matrix. J. Cell Biol. *110*, 569–580.

Höger, T.H., Krohne, G., and Kleinschmidt, J.A. (1991). Interaction of *Xenopus* lamins A and L_{II} with chromatin *in vitro* mediated by a sequence element in the carboxy terminal domain. Exp. Cell Res. *197*, 280–289.

Höner, B., Shoeman, R.L., and Traub, P. (1991). Human immunodeficiency virus type 1 protease microinjected into cultured human skin fibroblasts cleaves vimentin and affects cytoskeletal and nuclear architecture. J. Cell Sci. *100*, 799–807.

Ingber, D.E. (1997). Tensegrity-the architectural basis of cellular mechanotransduction. Annu. Rev. Physiol. *59*, 575–599.

Jackson, D.A., and Cook, P.R. (1988). Visualization of a filamentous nucleoskeleton with a 23 nm axial repeat. EMBO J. *7*, 3667–3677.

Kamei, H. (1994). Relationship of nuclear invaginations to perinuclear rings composed of intermediate filaments in MIA PaCa-2 and some other cells. Cell Struct. Funct. *19*, 123–132.

Kaplan, A.H., and Swanstrom, R. (1991). Human immunodeficiency virus type 1 Gag proteins are processed in two cellular compartments. Proc. Natl. Acad. Sci. USA *88*, 4528–4532.

Karczewski, M.K., and Strebel, K. (1996). Cytoskeleton association and virion incorporation of the human immunodeficiency virus type 1 Vif protein. J. Virol. *70*, 494–507.

Konvalinka, J., Litterst, M.A., Welker, R., Kottler, H., Rippmann, F., Heuser, A.M., and Kräusslich, H.-G. (1995). An active-site mutation in the human immunodeficiency virus type 1 proteinase (PR) causes reduced PR activity and loss of PR-mediated cytotoxicity without apparent effect on virus maturation and infectivity. J. Virol. *69*, 7180–7186.

Kräusslich, H.-G. (1991). Human immunodeficiency virus protease dimer as a component of the viral polyprotein prevents particle assembly and viral infectivity. Proc. Natl. Acad. Sci. USA *88*, 3213–3217.

Lelievre, S., Weaver, V.M., and Bissell, M.J. (1996). Extracellular matrix signaling from the cellular membrane skeleton to the nuclear skeleton: a model of gene regulation. Recent Prog. Horm. Res. *51*, 417–432.

Lindhofer, H., Nitschko, H., Wachinger, G., and von der Helm, K. (1993). Human-immunodeficiency-virus (HIV) proteinase in HIV-infected cell culture: dual intracellular effects in the absence or presence of inhibitor. In: Proteolysis and Protein Turnover, ed. J.S. Bond, and A.J. Barrett, London: Portland Press, 219–224.

Luderus, M.E.E., den Blaauwen, J.L., de Smit, O.J.B., Compton, D.A., and van Driel, R. (1994). Binding of matrix attachment regions to lamin polymers involves single-stranded regions and the minor groove. Mol. Cell. Biol. *14*, 6297–6305.

Maniotis, A.J., Chen, C.S., and Ingber, D.E. (1997). Demonstration of mechanical connections between integrins, cytoskeletal filaments, and nucleoplasm that stabilize nuclear structure. Proc. Natl. Acad. Sci. USA *94*, 849–854.

Meng, J.-j., Khan, S., and Ip, W. (1996). Intermediate filament protein domain interactions as revealed by two-hybrid screens. J. Biol. Chem. *271*, 1599–1604.

Menz, K., Radomski, N., and Jost, E. (1996). INMP, a novel intranuclear matrix protein related to the family of intermediate filament-like proteins: molecular cloning and sequence analysis. Biochim. Biophys. Acta *1309*, 14–20.

Nagy, K., Young, M., Baboonian, C., Merson, J., Whittle, P., and Oroszlan, S. (1994). Antiviral activity of human immunodeficiency virus type 1 protease inhibitors in a single cycle of infection: evidence for a role of protease in the early phase. J. Virol. *68*, 757–765.

Nelson, W.J., Vorgias, C.E., and Traub, P. (1982). A rapid method for the large scale purification of the intermediate filament protein vimentin by single-stranded DNA-cellulose affinity chromatography. Biochem. Biophys. Res. Commun. *106*, 1141–1147.

Padros, M.R., Giles, D.M., and Suarez, M.D. (1997). Intranuclear network of 3–5 nm and 8–10 nm fibers in EL-4 lymphoma cells. Cell. Biol. Int. *21*, 367–373.

Pyrpasopoulou, A., Meier, J., Maison, C., Simos, G., and Georgatos, S. (1996). The lamin B receptor (LBR) provides essential chromatin docking sites at the nuclear envelope. EMBO J. *15*, 7108–7119.

Rosé, J.R., Babé, L.M., and Craik, C.S. (1995). Defining the level of human immunodeficiency virus type 1 (HIV-1) protease activity required for HIV-1 particle maturation and infectivity. J. Virol. *69*, 2751–2758.

Sambrook, J., Fritsch, E.F., and Maniatis, T. (1989). Molecular Cloning. A Laboratory Manual. Cold Spring Harbor, NY: Cold Spring Harbor Laboratory.

Sarria, A.J., Lieber, J.G., Nordeen, S.K., and Evans, R.M. (1994). The presence or absence of a vimentin-type intermediate filament network affects the shape of the nucleus in human SW-13 cells. J. Cell Sci. *107*, 1593–1607.

Sarria, A.J., Nordeen, S.K., and Evans, R.M. (1990). Regulated expression of vimentin cDNA in cells in the presence and absence of a preexisting vimentin filament network. J. Cell Biol. *111*, 553–565.

Sarria, A.J., Sankhavaram, R.P., and Evans, R.M. (1992). A functional role for vimentin intermediate filaments in the metabolism of lipoprotein-derived cholesterol in human SW-13 cells. J. Biol. Chem. *267*, 19455–19463.

Seelmeier, S., Schmidt, H., Turk, V., and von der Helm, K. (1988). Human immunodeficiency virus has an aspartic-type protease that can be inhibited by pepstatin A. Proc. Natl. Acad. Sci. USA *85*, 6612–6616.

Shoeman, R.L., Hartig, R., and Traub, P. (1999). Characterization of the nucleic acid binding region of the intermediate filament protein vimentin by fluorescence polarization. Biochemistry *38*, 16802–16809.

Shoeman, R.L., Höner, B., Mothes, E., and Traub, P. (1992). Potential role of the viral protease in human immunodeficiency virus type 1 associated pathogenesis. Med. Hypotheses *37*, 137–150.

Shoeman, R.L., Höner, B., Stoller, T.J., Kesselmeier, C., Miedel, M.C., Traub, P., and Graves, M.C. (1990a). Human immunodeficiency virus type 1 protease cleaves the intermediate filament proteins vimentin, desmin and glial fibrillary acidic protein. Proc. Natl. Acad. Sci. USA *87*, 6336–6340.

Shoeman, R.L., Hüttermann, C., and Traub, P. (1996). Human immunodeficiency virus type 1 protease (HIV-1 PR)-mediated changes in nuclear architecture correlate with and are probably caused by cleavage of vimentin. Mol. Biol. Cell *7S*, 554a.

Shoeman, R.L., Kesselmeier, C., Mothes, E., Höner, B., and Traub, P. (1991). Non-viral substrates for human immunodeficiency virus type 1 protease. FEBS Lett. *278*, 199–203.

Shoeman, R.L., Mothes, E., Kesselmeier, C., and Traub, P. (1990b). Intermediate filament assembly and stability *in vitro*: effect and implications of the removal of head and tail domains of vimentin by the human immunodeficiency virus type 1 protease. Cell. Biol. Int. Rep. *14*, 583–594.

Shoeman, R.L., Sachse, C., Höner, B., Mothes, E., Kaufmann, M., and Traub, P. (1993). Cleavage of human and mouse cytoskeletal and sarcomeric proteins by human immunodeficiency virus type 1 protease. Actin, desmin, myosin and tropomyosin. Am. J. Pathol. *142*, 221–230.

Spann, T.P., Moir, R.D., Goldman, A.E., Stick, R., and Goldman, R.D. (1997). Disruption of nuclear lamin organization alters the distribution of replication factors and inhibits DNA synthesis. J. Cell Biol. *136*, 1201–1212.

Thomas, E.K., Conelly, R.J., Pennathur, S., Dubrovsky, L., Haffar, O.K., and Bukrinsky, M.I. (1996). Anti-idiotypic antibody to the V3 domain of gp120 binds to vimentin: a possible role of intermediate filaments in the early steps of HIV-1 infection cycle. Virol. Immunol. *9*, 73–87.

Traub, P., Mothes, E., Shoeman, R., Kühn, S., and Scherbarth, A. (1992a). Characterization of the nucleic acid-binding activities of the isolated amino-terminal head domain of the intermediate filament protein vimentin reveals its close relationship to the DNA-binding regions of some prokaryotic single-stranded DNA-binding proteins. J. Mol. Biol. *228*, 41–57.

Traub, P., Perides, G., Kühn, S., and Scherbarth, A. (1986). Interaction *in vitro* of non-epithelial intermediate filament proteins with histones. Z. Naturforsch *42C*, 47–63.

Traub, P., Scherbarth, A., Wiegers, W., and Shoeman, R.L. (1992b). Salt-stable interaction of the amino-terminal head region of vimentin with the α-helical rod domain of cytoplasmic intermediate filament proteins and its relevance to protofilament structure and filament formation and stability. J. Cell Sci. *101*, 363–381.

Traub, P., and Shoeman, R.L. (1994). Intermediate filament proteins: cytoskeletal elements with gene regulatory function? Int. Rev. Cytol. *154*, 1–103.

Wang, Q., Shoeman, R., and Traub, P. (2000). Identification of the amino acid residues of the amino terminus of vimentin responsible for DNA binding by enzymatic and chemical sequencing and analysis by MALDI-TOF. Biochemistry *39*, 6645–6651.

Wang, X., and Traub, P. (1991). Resinless section immunogold electron microscopy of karyo-cytoskeletal frameworks of eukaryotic cells cultured *in vitro*. Absence of a salt-stable nuclear matrix from mouse plasmacytoma MPC-11 cells. J. Cell Sci. *98*, 107–122.